PN-DIODE TRANSDUCED 3.7-GHZ SILICON RESONATOR

Eugene Hwang and Sunil A. Bhave
Cornell University, Ithaca, NY, USA

ABSTRACT

We present in this paper the design and fabrication of a homogeneous silicon micromechanical resonator actuated using forces acting on the immobile charge in the depletion region of a symmetrically doped pn-diode. The proposed resonator combines the high quality factor (Q) of air-gap transduced resonators with the frequency scaling benefits of internal dielectrically transduced resonators. Using this transduction method, we demonstrate a thickness longitudinal mode micromechanical resonator with Q ~ 18,000 at a resonant frequency of 3.72 GHz, yielding an $f \cdot Q$ product of 6.69 x 10^{13}, which is close to the intrinsic $f \cdot Q$ product of 10^{14} for (100)-Si.

INTRODUCTION

The potential of micromechanical devices as high quality factor resonators has been recognized since the seminal paper by Nathanson et al. describing the resonant gate transistor [1]. Continued research in micromechanical resonators has since pushed resonant frequencies into the multi-GHz range while improving transduction efficiency and reducing motional impedance. Recent developments include fabrication techniques to create large aspect-ratio resonators by minimizing the gap width and maximizing the transduction area of air-gap transduced silicon resonators [2], [3] or using different transducer (capacitive or piezoelectric) materials in a composite resonator structure [4], [5], [6]. While these methods show promise for increasing the transducer efficiency, there are certain limitations associated with each. High aspect-ratio air-gap resonators have the potential for high quality factor due to the homogeneous resonator structure, but are limited due to low fabrication yield and reliability. Piezoelectric transducers [5] have demonstrated low motional impedances, but the greater inherent material losses compared to silicon limit the quality factor of these devices. The use of high-K dielectrics [4], [6] increase the transduction efficiency over air-gap transduced resonators by bolstering the dielectric constant of the capacitive transducer and have the added benefit of increased reliability, but interface losses between the resonator body and transducer materials – especially when the transducer is placed at locations of maximum strain – limit the quality factor of these devices.

In this paper, we present a method of transduction that seeks to combine the strengths of the previously mentioned transduction methods to design high quality factor resonators at gigahertz frequencies. This is done by actuating mechanical motion using the force acting on the immobile charge within the depletion region of a pn-diode. Similar depletion-layer actuation has been observed with atomic force microscopy using gold-silicon Schottky diodes to excite resonance in cantilever beams [7] and to study electrostriction in silicon [8] at low frequencies. Due to the internal nature of depletion-layer transduction (i.e., the force is applied within the resonator), such resonators can be efficiently actuated at high frequencies when the junction is placed at optimal locations within the resonator. In this paper, we present the theory of operation for the pn-diode transduced micromechanical resonators and show experimental results for thickness longitudinal mode resonators (i.e., FBAR mode [9]) – pictured in Figure 1 – to validate our claims. Future work and implications are discussed in the conclusion.

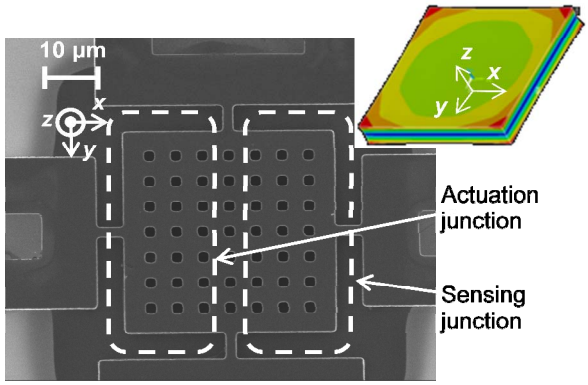

Figure 1: *SEM of the 40 µm × 40 µm pn-diode transduced micromechanical resonator. The resonant frequency of 3.72 GHz is determined by the silicon device layer thickness (no electrodes or other mass loading layers). The thickness displacement amplitude of the resonant mode shape is shown in the inset plot. Etch holes are required for timed HF release.*

THEORY OF OPERATION

This work combines the theories of depletion layer actuation [7] and internal dielectric transduction [4]. We first find the force distribution within the resonator body. This force distribution arises from the electrostatic force acting on the immobile charge (i.e., donor/acceptor ions) within the depletion region of the pn-junction. This is shown graphically in Fig. 2. Assuming an abrupt symmetric junction profile, the expressions for the charge distribution $\rho(z)$, electric field $E_Z(z)$, and the force distribution $\partial F / \partial z$ are given by

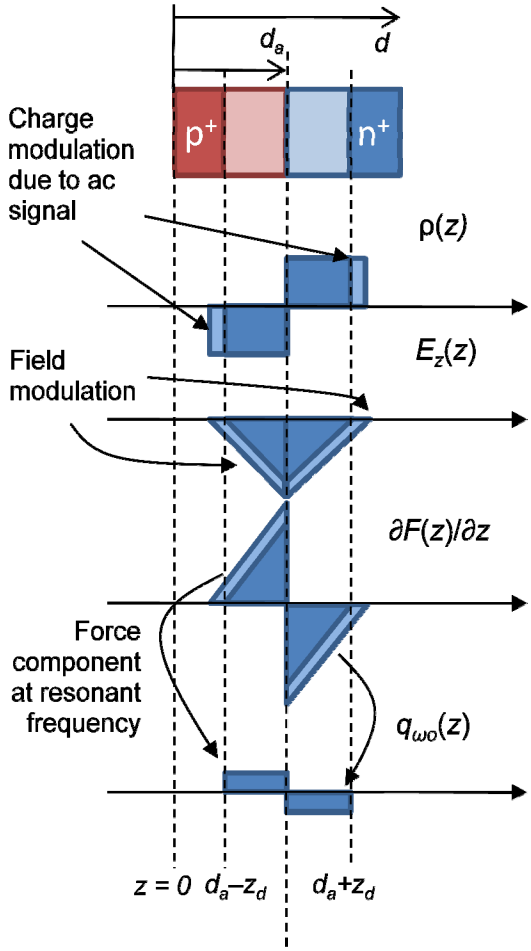

Figure 2: *Illustration of principle of actuation in the input junction showing the charge density ρ, electric field in the thickness direction E_z, and force component at resonant frequency $q_{\omega o}$ throughout the structure.*

$$\rho(z) = \begin{cases} -eNA_j, & -z_d < z < 0 \\ eNA_j, & 0 < z < z_d \end{cases} \tag{1}$$

$$E_z(z) = \begin{cases} -\frac{eNA_j}{\varepsilon_{si}\varepsilon_0}(z_d + z), & -z_d < z < 0 \\ \frac{eNA_j}{\varepsilon_{si}\varepsilon_0}(z - z_d), & 0 < z < z_d \end{cases} \tag{2}$$

$$\frac{\partial F}{\partial z} = \begin{cases} \frac{e^2N^2A_j}{\varepsilon_{si}\varepsilon_0}(z_d + z), & -z_d < z < 0 \\ \frac{e^2N^2A_j}{\varepsilon_{si}\varepsilon_0}(z - z_d), & 0 < z < z_d \end{cases} \tag{3}$$

where e is the elementary charge, N is the symmetric doping concentration, ε_{si} is the relative permittivity of silicon, ε_0 is the permittivity of free space, A_j is the junction area, and $2z_d$ is the junction depletion width given by the expression

$$z_d(v_{in}) = \sqrt{\frac{\varepsilon_{si}\varepsilon_0}{eN}(\Phi_{bi} - V_{DC} - v_{in}(t))} \tag{4}$$

where Φ_{bi} is the junction built-in voltage.

Eq. (1)-(4) indicate that this function is strongly nonlinear with the input ac voltage described by $v_{in} = v_o e^{-j\omega_o t}$. If $v_o << \Phi_{bi} - V_{DC}$, then (3) can be linearized around the bias point, yielding the distributed force at the excitation frequency

$$q_{\omega_o}(z,t) = \begin{cases} \frac{(eN)^{3/2}A_j}{2\sqrt{\varepsilon_{si}\varepsilon_0(\Phi_{bi}-V_{DC})}} v_o e^{-j\omega_o t}, & -z_d < z < 0 \\ -\frac{(eN)^{3/2}A_j}{2\sqrt{\varepsilon_{si}\varepsilon_0(\Phi_{bi}-V_{DC})}} v_o e^{-j\omega_o t}, & 0 < z < z_d. \end{cases} \tag{5}$$

This force distribution yields the following equation of motion

$$\rho A\frac{\partial^2 u(z,t)}{\partial t^2} - bA\frac{\partial^3 u(z,t)}{\partial t \partial z^2} - EA\frac{\partial^2 u(z,t)}{\partial z^2} = q_{\omega_o}(z - d_a, t). \tag{6}$$

Here, ρ is the mass density, E is the Young's Modulus, b is the loss factor, d_a is the location of the actuation junction, A is the resonator cross-sectional area, and $u(z,t)$ is the displacement field within the resonator. This field can be written as $u(z,t) = U_o \cos\left(\frac{n\pi z}{d}\right) e^{-j\omega_o t}$. Note that from this point forward, the subscripts 'a' and 's' are used to differentiate between parameters of the actuation and sensing junctions, respectively. The spatial shift of the force distribution is necessary since the expressions for the force distribution assume the junction is located at $z = 0$. This shift does not change the analytical form of any of these expressions, only the ranges in which they apply. Multiplying (6) by the mode shape and integrating over the thickness d of the resonator allows us to find the electromechanical transduction efficiency of the actuation junction

$$\eta_a = \frac{2dA_j}{n\pi}\frac{eN_a}{z_{d0,a}} \sin\left(\frac{n\pi d_a}{d}\right) \sin^2\left(\frac{n\pi z_{d0,a}}{2d}\right) \tag{7}$$

where $z_{d0,a} = z_{d,a}(v_{in} = 0)$.

Using a two-port configuration, a similar pn-junction is used to sense the motion at the output (see Figure 1). The depletion region is mechanically modulated by the standing wave in the resonator, which results in an output current, much like that of a capacitively sensed micromechanical resonator. This motional current is given by

$$i_m = V_{j,s}\frac{\partial C_j}{\partial t} = \eta_s \dot{u}(z,t). \tag{8}$$

Assuming small displacement ($U_o << W_{d,s}$), we are able to find the capacitive sensing efficiency

$$\eta_s = \frac{\varepsilon_{si}\varepsilon_0(\Phi_{bi,s} - V_{DC,s})A_j}{2z_{d0,s}{}^2} \sin\left(\frac{n\pi d_s}{d}\right) \sin\left(\frac{n\pi z_{d0,s}}{d}\right). \tag{9}$$

Defining the motional impedance to be $R_X \equiv v_o/i_m$, this can be expressed as

$$R_X = \frac{n\pi A\sqrt{E\rho}}{2Q}\frac{1}{\eta_a\eta_s}, \text{ where } Q = \frac{L}{n\pi}\frac{\sqrt{E\rho}}{b}. \tag{10}$$

Eq. (7)-(10) show the strong dependence of the motional impedance on the junction locations and the depletion layer widths, similar to what is shown in [4].

Thus, the same intuition regarding placement of the transducer at minimum displacement locations (maximum strain locations) still holds. It is also true that the motional impedance will exhibit a minimum near frequencies where the depletion width approaches half of the acoustic wavelength. The rest of the Butterworth-Van Dyke model is obtained by using the expressions for L_X and C_X given by

$$L_X = \frac{\rho A d}{2}\frac{1}{\eta_a \eta_s},\ C_X = \frac{2d}{n^2\pi^2 EA}\eta_a\eta_s. \quad (11)$$

As is the case with other electrostatically actuated resonators, there is a static capacitance associated with the transducer. For this resonator, the static capacitance is equal to the depletion capacitance given by

$$C_o = \frac{\varepsilon_{si}\varepsilon_0 A_j}{2z_{d0}} = \sqrt{\frac{\varepsilon_{si}\varepsilon_0 eN}{(\Phi_{bi}-V_{DC})}}\frac{A_j}{2}. \quad (12)$$

This capacitance usually sets the sensitivity of the resonance in electrostatically transduced resonators, but the dual diode configuration used in the resonator may make possible some self-gain mechanism (e.g., BJT configuration) to boost the resonant signal, as demonstrated in air-gap FET sensing [10]. This will be investigated further in future work.

Note that the preceding analysis assumes quasi-static electrical behavior, i.e., the charge carriers are able to respond within a time much shorter than the period of the input stimulus. This requires both junctions to be in reverse bias where electrical dynamic behavior is governed by majority carriers. Dynamics in forward bias are governed by minority carriers, which respond much more slowly, thus involving a more detailed analysis that will be presented in future work.

FABRICATION

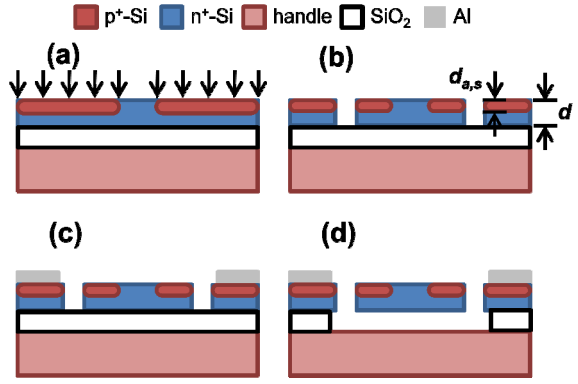

Figure 3: *(a) The 1.3 μm device layer of an SOI wafer is selectively doped using boron implantation and annealed to achieve the desired junction depth of 0.65 μm. (b) The device layer is etched to define the resonator and pads. (c) Aluminum is deposited and etched to define the interconnect and pad structure. (d) The device layer is released via timed HF etch.*

Device fabrication was performed at the Cornell Nanofabrication Facility following the steps outlined in Figure 3. Initially, a custom n^+ doped SOI wafer with 1.3 μm thick, (100)-oriented device layer with resistivity < 0.06 Ω-cm is used. The device layer is then selectively doped using boron ion implantation to define the actuation and sensing junctions and create ohmic contacts to metal interconnects. A subsequent rapid thermal anneal at 1100°C for 45 seconds is used for dopant activation and to create the junction at the desired depth of 0.65 μm. This is followed by a reactive ion etch of the device layer to define the resonator and anchors. Interconnect and pad structures are defined by sputter deposition and wet etching of 50 nm Cr (for adhesion and to prevent spiking) and 100 nm Al. The device is finally released using an HF etch.

EXPERIMENTAL RESULTS

High frequency measurements were completed using an RF network analyzer with 50 Ω terminations. These results were obtained using a two-port pseudo-differential measurement (i.e., unreleased diode of same area was fabricated next to device) with on-chip SOT de-embedding. The transmission magnitude data is shown in Figure 5, indicating a mechanical quality factor of approximately 18,000 in vacuum for the fundamental mode. Other than the device featured in this figure, we have successfully measured at least five other resonators all demonstrating $R_X < 3$ kΩ and $Q > 15{,}000$. Temperature measurements were also performed using a Lakeshore cryogenic vacuum probe station. Figure 6 shows the temperature dependence of the resonant frequency, indicating a TC_f = -9.72 ppm/°C over the temperature range of 5 - 75°C. This is about 3× lower than typical silicon micromechanical resonators and is consistent with previous work concerning degenerate doping and temperature compensation, as reported in [11], [12].

CONCLUSIONS

This work combines the pioneering work of [4] and [7] to develop a micromechanical resonator with the benefits of high quality factor at GHz frequencies. This is made possible by the use of pn-diode transduction, which allows efficient transduction at high frequencies without using a separate transducer material. Using this method, we present a thickness longitudinal mode micromechanical resonator with resonant frequency of 3.72 GHz and an $f{\cdot}Q$ product of 6.69 x 10^{13}. This is close to the theoretical limit in (100)-Si of ~10^{14} as predicted by [13]. In addition, the proposed device results in a CMOS-compatible fabrication process and higher device yield as compared to traditional air-gap or dielectrically transduced resonators.

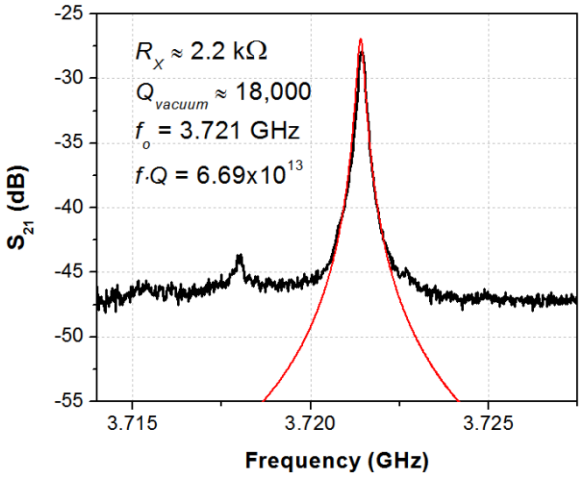

Figure 5. *Pseudo-differential transmission magnitude plot of pn-diode resonator shown in Figure 1 in vacuum after SOT de-embedding demonstrating Q ~ 18,000 at 3.72 GHz. Red trace shows fit with equivalent circuit model from (10)-(11). A bias voltage of -5V is applied to each junction.*

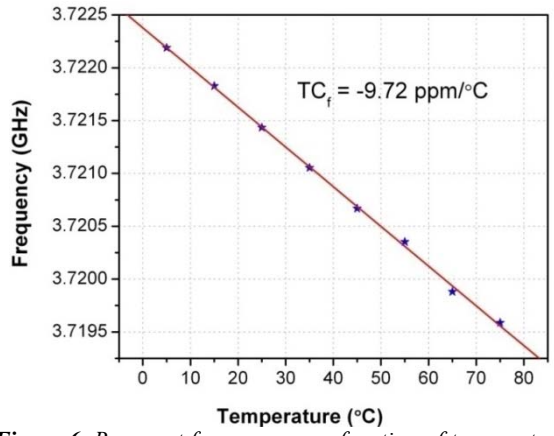

Figure 6. *Resonant frequency as a function of temperature. This figure shows a linear dependence with a temperature coefficient of -9.72 ppm/°C over a temperature range of 5 - 75°C.*

These benefits make pn-diode transduced micromechanical resonators possible candidates for use in chip-scale spectrum analyzers and ultra-lightweight MEMS-enabled radios.

ACKNOWLEDGEMENTS

The authors wish to thank DARPA and ARL for supporting this research. In particular, Dr. Ron Polcawich of ARL helped with device fabrication. The authors would also like to acknowledge the staff of the Cornell Nanofabrication Facility for additional assistance with device fabrication.

REFERENCES

[1] H. C. Nathanson, W. E. Newell, R. A. Wickstrom, J. R. Davis, Jr., "The resonant gate transistor," *IEEE Trans. Elec. Dev.*, **14** (3), pp. 117-133 (1967).

[2] S. Pourkamali, A. Hashimura, R. Abdolvand, G. K. Ho, A. Erbil, F. Ayazi, "High-Q single crystal silicon HARPSS capacitive beam resonators with self-aligned sub-100-nm transduction gaps," *IEEE/ASME JMEMS*, **12** (4), pp. 487-496 (2003).

[3] L. Hung, Z. A. Jacobson, Z. Ren, A. Javey, C. T.-C. Nguyen, "Capacitive transducer strengthening via ALD-enabled partial gap filling," *Hilton Head 2008*, pp. 208-211.

[4] D. Weinstein, S. A. Bhave, "Internal dielectric transduction of a 4.5 GHz silicon bar resonator," *IEDM 2007*, pp. 415-418.

[5] G. Piazza, P. J. Stephanou, A. P. Pisano, "Piezoelectric aluminum nitride vibrating contour-mode MEMS resonators," *IEEE/ASME JMEMS*, **15** (6), pp. 1406-1418 (2006).

[6] Y.-W. Lin, S.-S. Li, Y. Xie, Z. Ren, C. T.-C. Nguyen, "Vibrating micromechanical resonators with solid dielectric capacitive transducer gaps," *IEEE IFCS 2005*, pp. 128-134.

[7] J. H. T. Ransley, C. Durkan, A. A. Seshia, "A depletion layer actuator," *Transducers '07*, pp. 1393-1396.

[8] S. W. P. van Sterkenburg, "The electrostriction of silicon and diamond," *J. Phys. D: Appl. Phys.*, **25** (6), pp. 996-1003, (1992).

[9] R. Ruby, P. Bradley, J. Larson III, Y. Oshmyansky, D. Figueredo, "Ultra-miniature high-Q filters and duplexers using FBAR technology," *ISSCC 2001*, pp. 120-121, 438.

[10] D. Grogg, M. Mazza, D. Tsamados, A. M. Ionescu, "Multi-gate vibrating–body field effect transistor (VB-FETs)," *IEDM 2008*, pp. 663-666.

[11] A. K. Samarao, F. Ayazi, "Temperature compensation of silicon micromechanical resonators via degenerate doping," to be presented at *IEDM 2009*.

[12] P. Csavinszky, N. G. Einspruch, "Effect of doping on elastic constants of silicon," *Phys. Rev. A*, **132** (6), pp. 2434-2440 (1963).

[13] R. Tabrizian, M. Rais-Zadeh, F. Ayazi, "Effect of phonon interactions on limiting the *f.Q* product of micromechanical resonators," *Transducers '09*, June 21-25, 2009, pp. 2131-2134.